332.18
R14

An approach to the study of mid-level vision in the alert macaque monkey

Keith P. Purpura, Jonathan L. Baker, Jae-Wook Ryou, Jonathan D. Victor
Division of Systems Neurology and Neuroscience, Feil Family Brain and Mind Research Institute, Weill Cornell Medical College, New York, NY

Introduction and Motivation

Mid-level Vision Early visual cortex in primates transforms the activity in the retinogeniculate pathway into signals that higher cortical areas use for making inferences about the surfaces, objects and movements. A complete description of the nature of these transformations at the mid-level of visual hierarchy (V1, V2, V3 and V4: V1-4) remains a central goal of visual neuroscience. As these regions are tightly interconnected and nearly simultaneously active, it is likely that areas V1-4 interact to utilize spatial correlations of multiple orders to locate and characterize edges, patches and corners. We are therefore interested in characterizing how single neurons and local groups are *tuned to spatial correlations* in V1-4 in the awake monkey. Analysis of tuning functions for well-defined (and independent) perceptual axes of spatial correlation will provide evidence for and definition of mechanisms of spatial integration within V1-4 that are sensitive to the order, strength and sign of local spatial statistics. Neuronal activity in mid-level visual areas that encodes higher-order spatial correlations has been described in the anesthetized monkey (Purpura et al., 1994; Freeman et al., 2013; Yu et al., 2015) and in humans using fMRI (Beason-Held et al., 1998; Freeman et al., 2013).

Framework for the Study of Mid-level Vision

V1-4 are composed of well-defined neuroanatomical modules, each with distinct visual neurophysiological properties. In order to study this set of areas simultaneously it is necessary to employ multi-microelectrode technology, and to utilize sets of visual stimuli that can produce interpretable responses from across V1-4, visual areas with a wide range of receptive field sizes, positions and tunings for spatial frequency, orientation and luminance. The stimuli used here consist of black-and-white textures that are drawn from a domain specified by a 10-parameter image space that determines black/white balance and nearest-neighbor correlations (Victor and Conte, 2012). These stimuli have been well-characterized psychophysically, capture informative aspects of natural scenes (Tkačik et al., 2010; Hermundstad et al., 2014) and have been used recently to determine how V1 and V2 contribute to the encoding of local elements of form and shape in the anesthetized monkey (Yu et al., 2015; Victor et al., SfN2015, 332.15). Psychophysical studies suggest that this texture space is represented in two ways: in an opponent fashion with neurons responding monotonically along preferred axes (Conte et al., 2015), and in a distributed one, where individual tuning functions are broader and not restricted to axes (Rizvi et al., 2014). The former accounts for threshold judgments, the latter accounts for judgments of suprathreshold saliency.

Tunings for spatial statistics in V1-4 of the awake monkey

We made multi-electrode recordings from the visual cortex of the awake monkey during a fixation task. During each trial, a series of images were flashed in the visual quadrant mapped to the region surrounding the lunate sulcus where the microelectrodes were placed. The images were samples from a 10-element texture space. Our preliminary studies with this approach show that stable, and well-isolated multi-area neural recordings can be obtained chronically over many consecutive months from V1-4, and that tuning for spatial correlation can be extracted from local activity.

Methods: multi-channel recording across V1-4

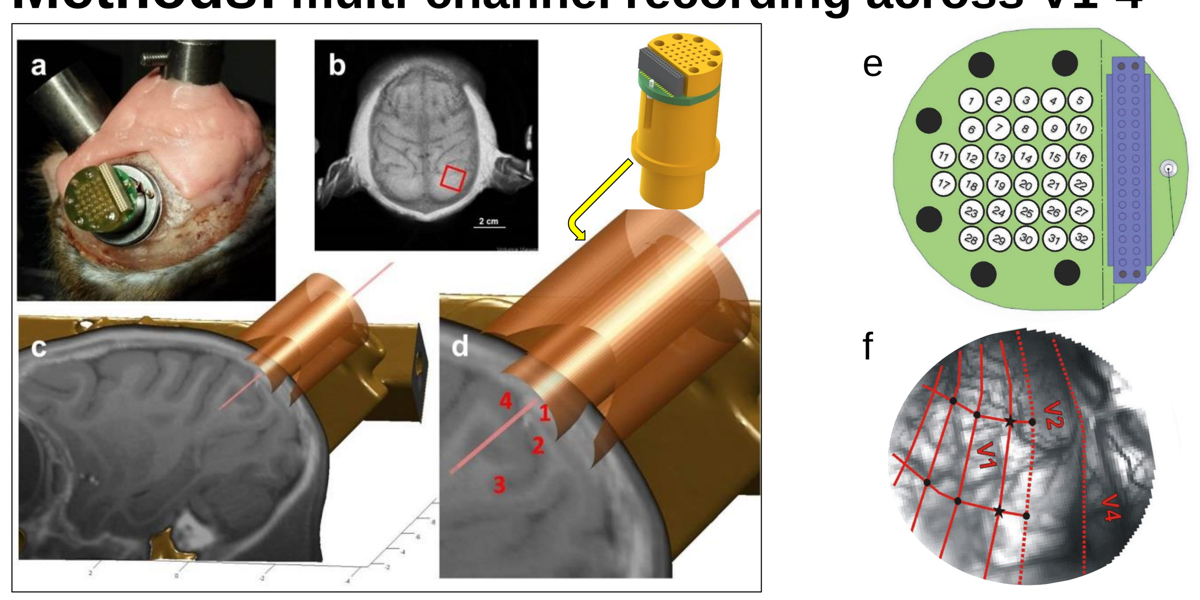

(a) Chronic implant viewed from the right side of the head. Posterior is to the left, anterior to the right of the image. Two Gray Matter Research recording chambers with microdrives (Gray Matter Research, Bozeman, MT) are implanted in the skull over the lunate sulcus in both hemispheres. The microdrive over the right lunate is exposed. (b) MRI of a monkey of comparable size to the animal used in this study. Red rectangle indicates the approximate position and size of the microdrive grid. (c) Sagittal section through a 3D model of the brain in stereotaxic space created from volumetric imaging data (MRI and CT). The two concentric cylinders placed over the lunate represent the extent of the craniotomy (outer cylinder) and the microdrive grid (inner cylinder). Red line: orientation of microelectrodes within the grid. (d) Detail of (c). The inset shows the 32-channel GMR microdrive. Numerals **1**, **2**, **3** and **4** are positioned over cortical areas V1, V2, V3 and V4, respectively (Gattass et al., 1988). (e) Layout of the 32-channel grid. Inter-grid spacing is 1.5 mm. (f) The dorsal surface of the cortex within the craniotomy underlying the grid is approximated here with an image from Ayzenshtat et al. (2012). Diameter of image covers ~11 mm of the cortical surface.

Additional Methods Non-Human Primate: 6 kg, male rhesus. Recordings: 32 Alpha-Omega microelectrodes, impedances range from 0.5-1.5 MΩ. Each microelectrode can be moved independently over a linear distance of ~20 mm. All neurophysiological signals were recorded with the RZ2 data acquisition system (Tucker Davis Technologies, Alachua, FL.) at a maximum sampling rate of ~25 KHz, bandwidth 0.1Hz - 8KHz. Eye Tracker: ASL E5000 (Applied Sciences Laboratories, Bedford, MA) infrared base-mounted system fitted with a telephoto lens, sampling rate 128 Hz. Eye tracker calibrated on a daily basis at the beginning of each day's recording session. Experimental Control: Visual stimuli and behavioral paradigms were generated and controlled by MATLAB (MathWorks, Natick, MA) Toolbox, MonkeyLogic running on a dedicated PC under Windows 7 with a streamlined system profile, and custom software written in MATLAB. Visual Display: Sony CRT, 85 Hz refresh subtending 22º H x 14º V at 100 cm from screen. Monkey was head restrained in a Crist primate chair (Crist Instrument Co, Hagerstown, MD). Monkey received a liquid reward (water or juice) if fixation was maintained within 1-2º of the fixation target for the duration of a trial.

Methods: 10 axes of the stimulus space

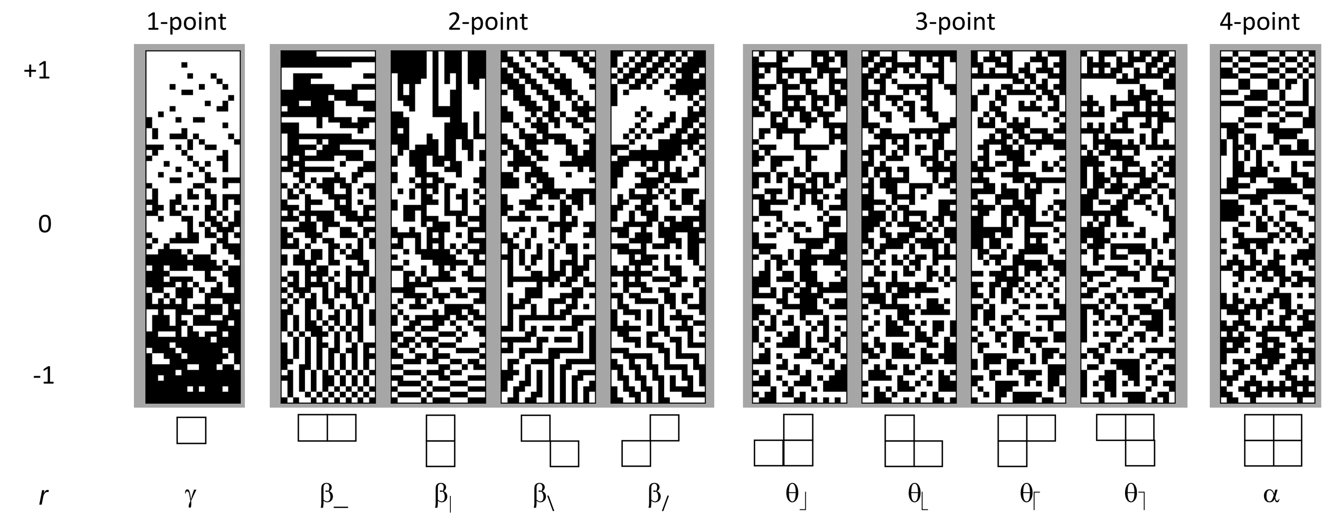

Image statistics. Spatial correlation: changes in strength and sign, r ranges from -1 to +1; 0 indicates random. Order of correlation: number of pixels in correlation. γ is a 1-point correlation, the difference in the fraction of bright vs. dark checks. The four β's are 2-point correlations, in the two cardinal and two diagonal directions. The four θ's are 3-point correlations. α is a 4-point correlation.

Methods: stimulation protocol, tuning for *r*

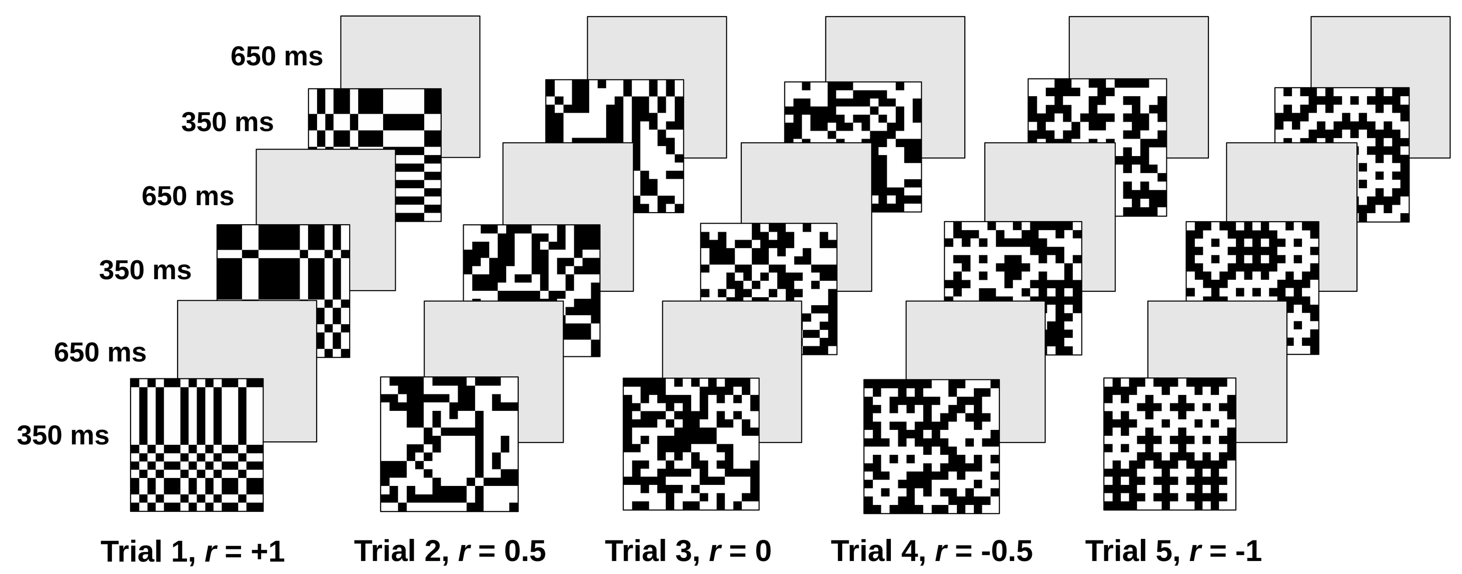

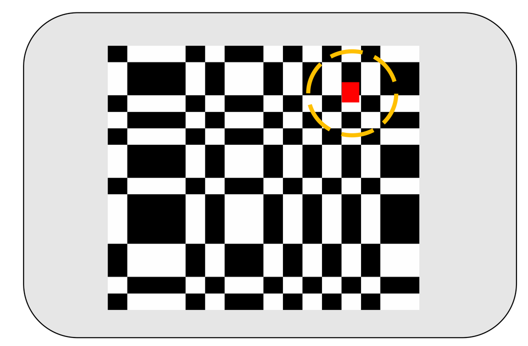

Smallest texture elements: 0.2º x 0.2º for some texture runs and 0.4º x 0.4º for other runs. Image region subtends 15º H x 13º V.

Trial Structure for a Texture Run Fixation target appears on a grey background. After a short period of stable fixation, a sequence of images (100% contrast) is presented (at most 3). If monkey maintains fixation within a window around the red target for the duration of the trial, the trial is scored correct and the monkey receives a reward. Typical runs include 240 trials. Each trial shows examples from one coordinate in the stimulus space. No stimulus is ever repeated. Shown here is a sequence of 5 trials that sample from 5 positions (degrees of spatial correlation) along the 4-point axis.

Multi-channel response dynamics across V1-4

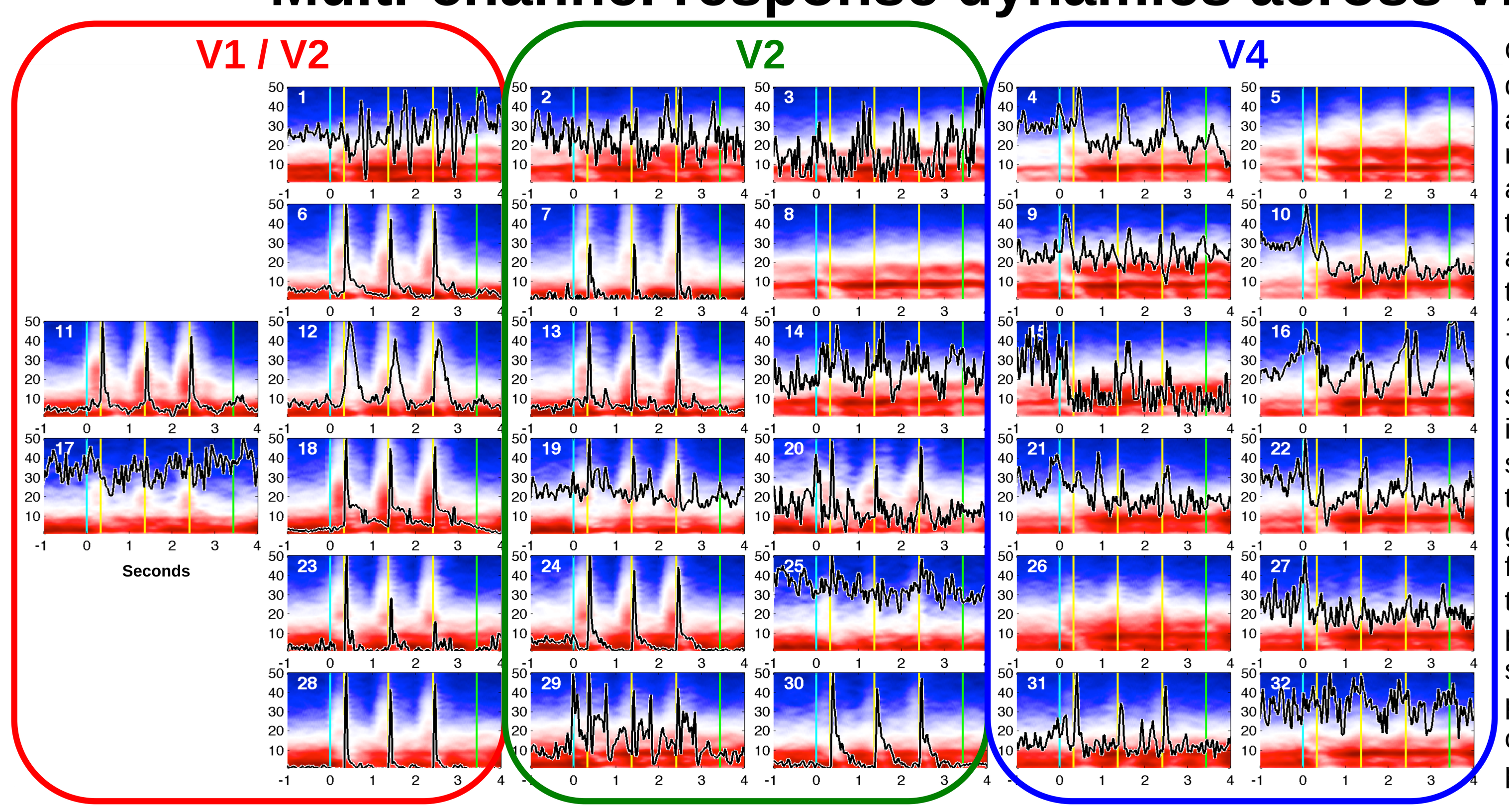

Overall responses dynamics are dominated by response transients as evident in the PSTHs of the multi-unit activity (MUA) recorded across the microdrive array during a texture run. Here 4-point textures are being presented. The responses to 9 values of r (ranging from -1 to 1) are averaged together. For each channel (number top left of each subplot), the cyan vertical line indicates the end of the period of stable fixation, the yellow lines mark the times of stimulus onset, and the green line indicates when the fixation target was turned from red to green. Only correct trials are presented. Spectrograms for the simultaneously recorded local field potentials are also shown for each channel (**red** indicates higher power, **blue** lower).

Multi-channel tuning across V1-4

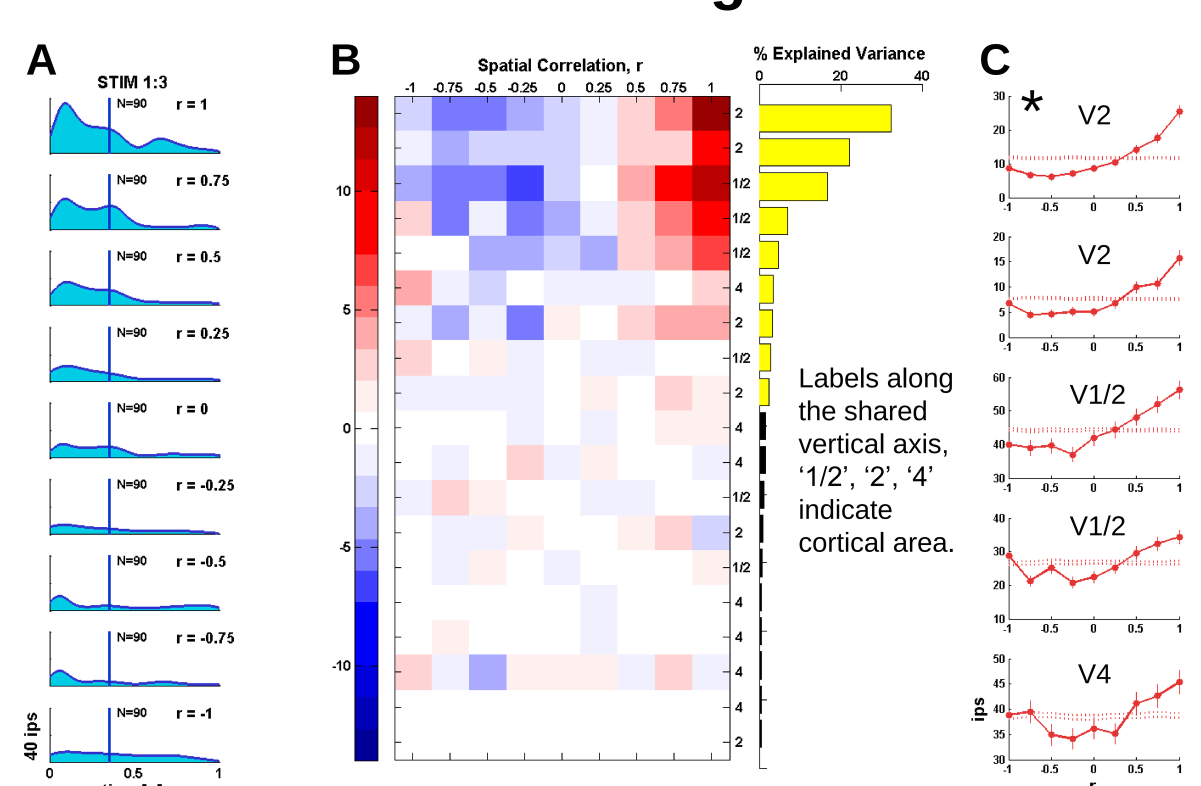

(A) LEFT: PSTHs for MUA recorded in V2 (*channel 30*) for a range of r values for 4-point textures (0.2º x 0.2º elements) during one texture run. Time zero represents when the texture was presented, lasting 350ms. The blue vertical line indicates the inter-stimulus gray screen period. Responses from the three consecutive stimuli shown in each correct trial are averaged together. Responses in this column are used for generating the tuning function at the top of the column **C** (*).
(B) CENTER: Dependence of firing rate on r during the 350 ms stimulus on-period plotted as the deviation of the rate from the average response obtained by shuffling across the r values. The channels are ordered by % of the variance in the rates explained by r (ANOVA). The significant values are colored yellow.
(C) RIGHT: The top five significant tuning functions in V1/V2, V2 and V4.

Tuning functions for *r* along several axes of the stimulus space

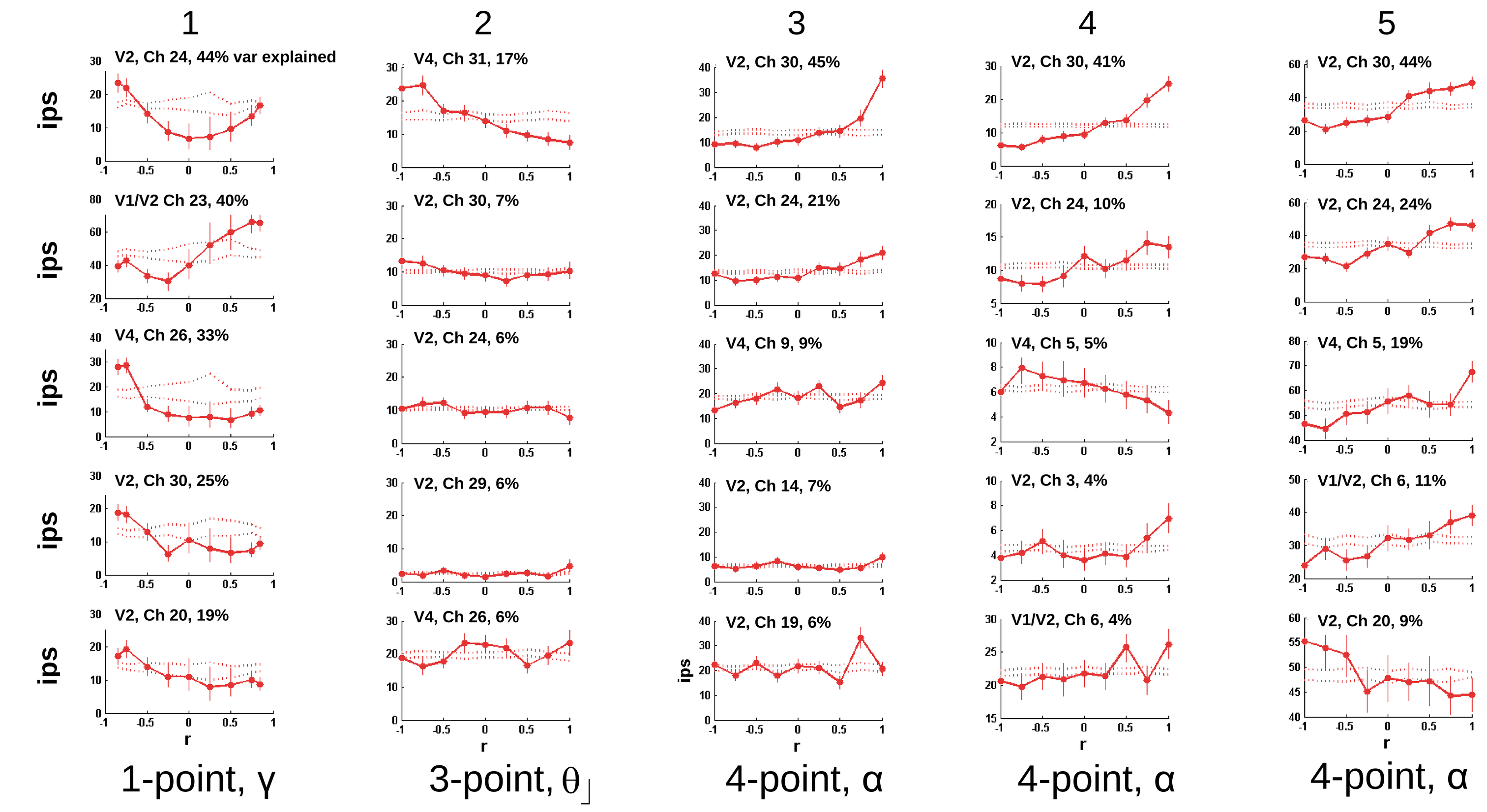

MUA from 5 unique texture runs (columns) in 5 different recording sessions. Dashed red lines indicate the mean rates obtained by shuffling the responses across r. Error bars are 95% CI for the rates at each r. ANOVA determined the importance of the factor r in explaining the variance for each channel in a run. The ordering in the column (top-to-bottom) is by % explained variance. The first column demonstrates tuning for luminance, i.e. the balance between black than white elements in the textures. Four out of the five sites show a bias towards darks (Yeh et al., 2009; Kremkow et al., 2014).

Summary of strength of modulation by *r* across the array

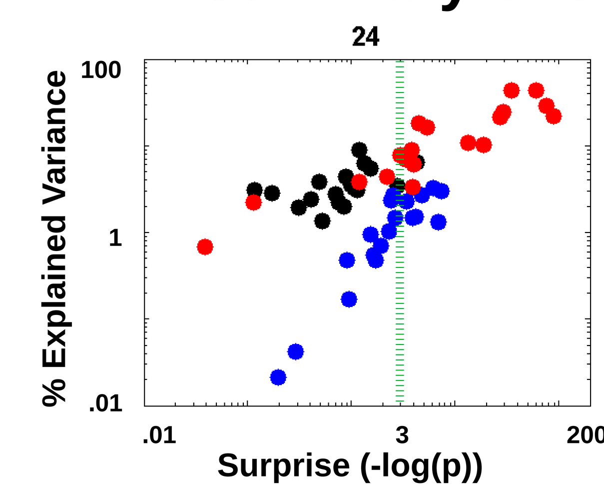

MUA's from each channel, for each texture run across 17 experimental sessions were combined into one population (N=433). An ANOVA was calculated with three factors: degree and sign of spatial correlation (r) (**RED**), the order of the stimulus presentation during each trial (**BLUE**), and an interaction term between these two factors (**BLACK**). The % of the variance explained by the factor for the recording is plotted against a log transform of the significance determined by an F-test. For many channels (e.g. Ch. 24, above), spatial correlation accounted for the largest fraction of variance, and its effect was significant ($p < 0.05$, to the right of the green line) in 30% of all the recordings (grid to the right). Stimulus order was a significant factor in 43% of the recordings. The interaction between spatial correlation and stimulus order was present only at chance levels

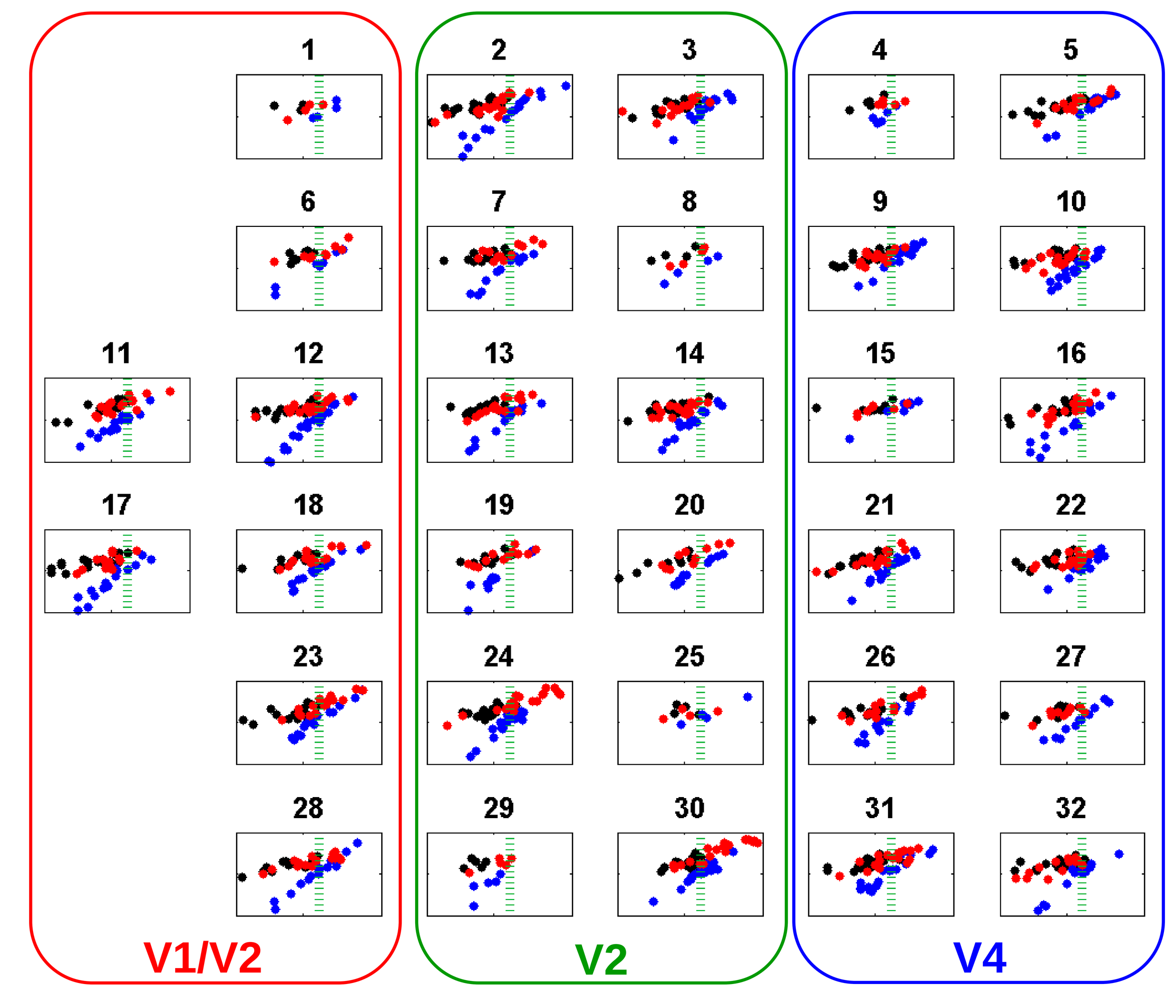

Summary and Conclusions

- **We show that chronic multi-channel microelectrode recordings from regions surrounding the lunate sulcus in the alert monkey provide a detailed view of processing stages in mid-level vision.**
- **Key to this approach is the utilization of a stimulus set that provides a common framework to investigate simultaneously a set of visual areas with diverse response properties.**
- **Tuning for the degree and sign of spatial correlation (*r*) was present at many locations across the array.**
- **MUA tuning for *r* was observed for all axes of the stimulus space studied to date (1-point, 3-point, and 4-point spatial correlations).**
- **Sequential presentations of the stimuli during fixation trials produce transient responses whose dynamics are modulated across the trials. The mechanisms underlying the generation of pattern specific responses are not significantly influenced by these response dynamics.**

Ayzenshtat, I., Gilad, A., Zurawel, G. & Slovin. H. (2012) Population response to natural images in the primary visual cortex encodes local stimulus attributes and perceptual processing. J. Neurosci., 32, 13971-13986
Beason-Held, L.L., Purpura, K.P., Krasuski, J.S., Maisog, J.M., Daly, E.M., Mangot, D.J., Desmond, R.E., Optican, L.M., Schapiro, M.B., & Van Meter, J.W. (1998) Cortical regions involved in texture perception: a fMRI study. Cognitive Brain Research, 7, 111-118.
Conte, M.M., Rizvi, S.M., & Victor, J.D. (2015) Approximately uniform isodiscrimination contours within a perceptual space of local image statistics. Vision Sciences Society Annual Meeting, St. Petersburg, FL, 2015.
Freeman, J., Ziemba, C.M., Heeger, D.J. Simoncelli, E.P., & Movshon, J.A. (2013) A functional and perceptual signature of the second visual area in primates. Nature Neurosci., 16, 974-981.
Gattass, R., Sousa, A.P. & Gross, C.G. (1988) Visuotopic organization and extent of V3 and V4 of the macaque. J. Neurosci., 8, 1831-1845.
Hermundstad, A. M., Briguglio, J.J., Conte, M.M., Victor, J.D., & Balasubramanian, V. (2014) Variance predicts salience in central sensory processing. eLife 3, doi:10.7554/eLife.03722.
Kremkow, J. , Jin, J., Komban, S.J., Wang, Y., Lashgari, R., Li, X., Jansen, M., Zaidi, Q., Alonso, J.M. (2014) Neuronal nonlinearity explains greater visual spatial resolution for darks than lights. Proc Natl Acad Sci U S A 111, 3170-3175.
Purpura, K.P., Victor, J.D., & Katz, E. (1994) Striate cortex extracts higher-order spatial correlations from visual textures. Proc. Natl. Acad. Sci. USA, 91, 8482-8486.
Rizvi, S.M., Conte, M.M. & Victor, J.D. (2014) Border salience reveals a curved global geometry of the perceptual space of local image statistics. Vision Sciences Society Annual Meeting, St. Petersburg, FL, 2014.
Tkačik, G., Prentice, J. S., Victor, J. D. & Balasubramanian, V. (2010) Local statistics in natural scenes predict the saliency of synthetic textures. Proc Natl Acad Sci U S A 107, 18149-18154.
Victor, J. D. & Conte, M. M. (2012) Local image statistics: maximum-entropy constructions and perceptual salience. J Opt Soc Am A Opt Image Sci Vis 29, 1313-1345.
Victor, J.D., Yu, Y., Thengone, D.J., Witztum, J., Nitzany, E.I., & Purpura, K.P. (2015) How do neurons in macaque visual cortex represent a high-dimensional perceptual space? Society for Neuroscience, Chicago, IL, 2015, 332.15.
Yeh, C. I., Xing, D. & Shapley, R. M. (2009) "Black" responses dominate macaque primary visual cortex v1. J Neurosci 29, 11753-11760.
Yu, Y., Schmid, A. M. & Victor, J. D. (2015) Visual processing of informative multipoint correlations arises primarily in V2. eLife 4, doi:10.7554/eLife.06604.